EurJOC

European Journal of Organic Chemistry

Chemistry Europe

European Chemical Societies Publishing

Accepted Article

Title: α-Amino Acids and α,β-Dipeptides Intercalated into Hydrotalcite: Efficient Catalysts in the Asymmetric Michael Addition Reaction of Aldehydes to N-Substituted Maleimides

Authors: José M Landeros, Carlos Cruz-Hernández, and Eusebio Juaristi

To be cited as: *Eur. J. Org. Chem.* 10.1002/ejoc.202100877

Link to VoR: https://doi.org/10.1002/ejoc.202100877

WILEY-VCH

10.1002/ejoc.202100877

WILEY-VCH

α-Amino Acids and α,β-Dipeptides Intercalated into Hydrotalcite: Efficient Catalysts in the Asymmetric Michael Addition Reaction of Aldehydes to *N*-Substituted Maleimides

José M. Landeros,*[a] Carlos Cruz-Hernández,[a] and Eusebio Juaristi*[a][b]

Abstract: In this work, a series of α-amino acids (L-Phe, D-Phe, L-Trp) and several α,β-dipeptides (H_2N-L-Val-*N*-Bn-β-Ala-COOH and H_2N-L-Leu-*N*-Bn-β-Ala-COOH) intercalated into hydrotalcite (Mg/Al, x = 0.333) were prepared by high speed ball milling (HSBM) assisted rehydration/reconstruction methods, followed of sonication and mechanical stirring. All organic-inorganic hybrid samples were characterized by powder X-ray diffraction (XRD) and FTIR-ATR spectroscopy. The catalytic activity of the resulting hydrotalcite-supported materials (natural and hybrid) was evaluated in the asymmetric Michael addition reaction of α,α-disubstituted-aldehydes to *N*-substituted-maleimides. Pristine (HTS), calcined (HTC) and water-reconstructed (HTR-l) hydrotalcite-derived materials exhibited very low catalytic activities, affording racemic mixtures of the anticipated Michael adduct. By contrast, hybrid materials showed better activities, especially HTR-α-amino acid catalysts afforded Michael products in up to 94% yield and with rather high enantioselectivity (enantiomeric ratio, e.r., up to 99:1) at room temperature under neat reaction conditions. The effect of solvents and Brønsted basic or acidic additives was evaluated using the best hybrid catalyst, HTR-L-Phe. In addition, recycling and reuse of the catalyst (up to 4 cycles) and large-scale experiments was successfully carried out.

Introduction

The asymmetric Michael addition reaction is widely recognized as one of the most important synthetic method for the formation of C–C bonds.[1] Indeed, during the last two decades, several reports have disclosed a wide range of its application in the synthesis of bioactive compounds by means of novel chiral organocatalysts.[2]

Among the plethora of Michael acceptors used in the stereoselective synthesis of fine chemicals, maleimides are particularly attractive for the preparation of chiral succinimides.[3] Indeed, enantioenriched succinimide scaffolds are key precursors of various natural products. Furthermore, chiral succinimides constitute a structural motif in effective drugs against HIV, as well as in antibacterial and antibiotic ingredients.[3,4] In this regard, a straightforward route to access enantioenriched chiral succinimides consists in the asymmetric Michael addition of α,α-disubstituted aldehydes to maleimides.[5,6] Following the seminal work of Córdova et al. in the organocatalyzed addition of α,α-disubstituted aldehydes to maleimides,[5] several chiral organocatalysts have been developed achieving high efficiency in this transformation. Such chiral organocatalysts comprise primary amines (PA) and 1,2-diamines,[6] bifunctional PA-guanidines, [7] bifunctional PA-thioureas,[8] amino acids and peptidic derivatives,[9] among others.[10] Despite of the high performance exhibited by these organocatalysts, most of them present drawbacks including the use of harmful solvents as reaction media, difficult separation from products and null recyclability, which reduces their sustainability, economic attractiveness and practical convenience. [11]

In order to overcome these issues, different approaches based on the principles of green chemistry have been applied in order to render organocatalysts more sustainable.[12] For example, green solvents such as ionic liquids and deep eutectic solvents,[13] or solvent-free conditions have been used to synthetize chiral succinimides.[9d] Furthermore, both covalently and non-covalently immobilized organocatalysts,[14,15] represent advantages such as easy recovery and reuse of the heterogenized catalyst. In this regard, Szőllősi *et al*. reported a series of chiral 1,2-diamines supported on polyester resin by means of sulfonamide linkers, affording the corresponding chiral succinimides in high enantioselectivity (up to 97% *ee*) even after 5 cycles; nevertheless, a significant decrease in conversion was observed throughout the cycles.[14] Very recently, Szőllősi et al. reported the use of L-proline adsorbed on the solid surface of diverse inorganic oxides and ion exchanger layered materials, where Laponite RD (synthetic cationic exchanger layered magnesia-silicate) afforded the best results in the Michael addition of carbonyl compounds to β-nitrostyrenes using the mixture of solvents chloroform:isopropanol, 9:1.[15] As part of this study, hydrotalcite was evaluated as additive affording excellent conversion (>99% yield). Nevertheless, the Michael addition reactions proceeded with low diastereo- (70% ds) and enantioselectivity (64% *ee*).

In view of the above precedents, we envisioned the development of an alternative way to incorporate amino acids and peptides into the interlaminar space of hydrotalcite by means of the reconstruction method, rather than by surface adsorption. It was anticipated that this strategy could provide an augmented catalytic effect in the confined space rendered by the layered material.[16]

[a] Dr. J.M. Landeros, Dr. C. Cruz-Hernández, Prof. Dr. E. Juaristi
Departamento de Química
Centro de Investigación y de Estudios Avanzados, Instituto Politécnico Nacional
Avenida IPN # 2508, 07360 Ciudad de México, Mexico.
E-mail: ejuarist@cinvestav.mx and/or jose.landeros@cinvestav.mx
http://www.relaq.mx/RLQ/EusebioJuaristi.html

[b] Prof. Dr. E. Juaristi.
El Colegio Nacional
Luis González Obregón 23, Centro Histórico, 06020 Ciudad de México, Mexico.

Supporting information for this article is given via a link at the end of the document.

Hydrotalcites (HT's) are natural anionic clays with lamellar structure.[17] Hydrotalcite-derived materials exhibit unique properties with tunable structural elements and potential biocompatibility, which are useful in applications such as drug carriers in medicine,[18] as well as in catalysis.[19] Hydrotalcite-type materials present the general formula $[M^{2+}_{1-x}M^{3+}_{x}(OH)_2]^{x+}(A^{n-})_{x/n}\cdot mH_2O$, where x ($0.2 \le x \le 0.33$) corresponds to the molar ratio $M^{2+}/(M^{3+} + M^{2+})$ of metal ions in the brucite layers, m is water of coordination and (A^{n-}) is the compensating anion in the interlayer space that is required to balance the electrical charges.[17a]

An interesting property of any HT-type material is the so-called "memory effect", that refers to its calcination (at ca. 450-600 ºC) to form mixed oxides of metals with the concomitant collapse of the interlaminar space, so that when the resulting oxides are exposed to water (vapor or liquid) this triggers the rehydration and reconstruction of the interlaminar space of hydrotalcite structure but now with H_2O and OH^- hydroxide as compensation anion, modifying the original basic properties.[20] When the water of rehydration is accompanied by organic anions (or biomolecules), these can be intercalated to some extent into the interlamellar space during the reconstruction process, forming organic-inorganic hybrid nanomaterials.[17] Indeed, several synthetic methodologies have been developed to incorporate biomolecules and organic guest into hydrotalcite.[21] In particular, the intercalation of amino acids and peptides into HT materials involve coprecipitation,[22] ion exchange[23] and reconstruction methods,[24] commonly assisted by ultrasound irradiation or mechanochemical activation.[25]

While several examples have been reported concerning the intercalation of amino acids and their derivatives into hydrotalcites,[22-25] to date very few examples have been reported regarding the use of amino acids and peptides intercalated into hydrotalcites as hybrid catalysts in asymmetric aldol and Michael addition reactions.[22j,23h,24c,24e,25b] In this regard, Choudary and co-workers reported several asymmetric C–C bond forming reactions catalyzed by L-proline anchored to HT (Mg/Al). This catalytic material was prepared by means of anion exchange and coprecipitation methods.[22j] Disappointingly, Michael addition of diethyl malonate to cyclohexenone catalyzed by this modified HT afforded the addition product in low yield (40%) and essentially null enantioselectivity.

On the other hand, Pitchumani and co-workers immobilized L-proline (L-Pro) into the interlaminar space of hydrotalcite (Mg/Al, 3:1) by means of the reconstruction method.[24e] The resulting hybrid catalyst HT-L-Pro was evaluated in the asymmetric Michael addition reaction of acetone to different β-nitrostyrenes, as well as nitromethane to several benzylideneacetones affording Michael adducts in modest to excellent yields, although with low to moderate enantioselectivity (up to 73:27 e.r.).

In this context, Medina and coworkers reported that during L-Leucine (L-Leu) intercalation into hydrotalcite (Mg/Al, 2:1) by reconstruction and ion exchange methods,[25b] parameters such as time, temperature and ultrasound irradiation play a major role in the extent of L-Leu immobilization. The resulting catalysts were evaluated in the asymmetric aldol reaction between different carbaldehydes and cyclohexanone, obtaining good to excellent yields, but low diastereoselectivity (up to 61:39 dr). Nevertheless, the reaction proceeded with good enantioselectivity after 7 days of reaction in DMSO/H_2O.[25b]

Upon consideration of the above results, it became apparent that there is still a need to develop synthetic strategies that result in the preparation of well-structured nanohybrid HT's that are efficient in asymmetric aldol and Michael addition reactions.

Taking into account this background information and motivated by the success achieved in our previous works employing both free and supported α,β-dipeptides as catalysts for asymmetric Michael addition of α,α-aldehydes to prochiral maleimides for the preparation of enantioenriched succinimides,[9d,e] herein we report the convenient preparation of various organic-inorganic hybrid catalysts based on the intercalation of α-amino acids (L- and D-phenylalanine, L-tryptophan) or α,β-dipeptides (H_2N-L-Val-β-*N*-Bn-Ala-COOH and H_2N-L-Leu-*N*-Bn-β-Ala-COOH) in reconstructed Mg/Al-hydrotalcite. These materials proved to be efficient catalysts in the asymmetric Michael addition reaction of α,α-aldehydes to prochiral *N*-substituted-maleimides. To the best of our knowledge, this is the first time than α-amino acids and α,β-dipeptides intercalated into hydrotalcite Mg/Al have been evaluated in the asymmetric Michael addition reaction of aldehydes to maleimides under solvent-free reaction conditions.

Results and Discussion

Synthesis of reconstructed hydrotalcite incorporating α-amino acids or α,β-dipeptides

Table 1 summarizes the conditions under which the synthesis of the organic-inorganic hybrid catalysts performed by the reconstruction method was carried out. In particular, the chemical synthesis was assisted by any one of three different procedures: a) magnetic stirring at ambient temperature for 20 h (method M1 in Table 1, entries 1-2), b) ultrasonic irradiation at 42 kHz for 90 min. (method M2 in Table 1, entry 3), and c) mechanochemical activation under High-Speed Ball milling (HSBM) at 25 Hz for 90 min (Method M3 in Table 1, entry 4). In addition, several variations involving alternative sequences of these methods were evaluated (Methods M4 to M6, Table 1, entries 5-8). Calcined Mg/Al mixed oxides (HTC) of commercial Mg/Al-hydrotalcite (HTS, x = 0.333) was used for all reconstructed samples. Typical in-water reconstructed hydrotalcite (HTR-l) was synthetized as benchmark material, using HTC and decarbonated water according to method M1, obtaining a hydrotalcite material with interlaminar water and HO^- anion (Table 1, entry 1).[20] In order to optimize the reconstruction conditions of hybrid materials, a mixture of L-phenylalanine (L-Phe) and HTC was adjusted to pH 13 with aqueous NaOH solution (to ensure that the amino acid species is present in ionic form). The resulting mixture was then subjected to the reconstruction conditions (Table 1, entries 2 to 6).

Materials HTR-M1, HTR-M2 and HTR-M3 were obtained by methods M1 to M3, respectively (Table 1, entries 2-4). Application of High Speed Ball milling followed by magnetic stirring afforded HTR-M4 material (Table 1, entry 5). Sonication followed by magnetic stirring provided material HTR-M5 (Table 1, entry 6) and HSBM followed by sonication, and then magnetic stirring were used to prepare HTR-M6 (Table 1, entry 7). Finally, material HTR-M7 was obtained by method M6, but with the initial reaction mixture adjusted to pH 11 (Table 1, entry 8).

Table 1. Procedures followed for the preparation of reconstructed hydrotalcites assisted by mechanical stirring, ultrasonic irradiation or mechanochemical activation.

Entry	Sample	Method[a]
1	HTR-I[b]	M1: Mechanical stirring for 20 h at rt.
2	HTR-M1	M1: Mechanical stirring for 20 h at rt.
3	HTR-M2	M2. Sonication for 90 min.[c]
4	HTR-M3	M3: HSBM at 25 Hz for 90 min.[d]
5	HTR-M4	M4: HSBM at 25 Hz for 90 min, then magnetic stirring for 20 h. [d][c]
6	HTR-M5	M5: Sonication for 60 min, then magnetic stirring for 20 h.[c]
7	HTR-M6	M6: HSBM at 25 Hz for 90 min, then sonication for 90 min, followed by mechanical stirring for 20 h at rt.[d][c]
8	HTR-M7[e]	M6: HSBM at 25 Hz for 90 min, then sonication for 90 min, followed of mechanical stirring for 20 h at rt.[e]

[a] Experimental conditions: 0.56 g (*ca.*1.6 mmol) of calcined hydrotalcite (HTC), L-phenylalanine (0.46 g, 2.8 mmol) and aqueous NaOH (1% w/w), in order to adjust to pH 13); this protocol was followed for all organic-inorganic samples. Decarbonated water (20 mL) was used as reaction media with magnetic stirring and ultrasonic irradiation. [b] HTC and decabonated water were used. [c] Ultrasonic bath at a frequency of 42 kHz. [d] High-speed ball milling (HSBM) employing a jar of PTFE (15 mL, 2.0 cm diameter) and two milling balls with core of stainless steel and a cover of PTFE (1 cm diameter, mass 1.757 g), under wet conditions. [e] Reaction mixture was adjusted to pH 11.

Figure 1 shows powder XRD patterns of pristine (HTS), calcined (HTC) and reconstructed (HTR-M1 to HTR-M7) hydrotalcites that were prepared by the different methods detailed in Table 1. HTS samples exhibit typical diffraction patterns, which can be divided in two groups: i) symmetric and sharp reflection with high intensity at low 2θ angle (11.6º, 23.3º and 34.8º), corresponding to basal planes (003), (006) and (009), indicating good crystallinity, and ii) asymmetric and broad reflection at high 2θ angles (60.7º. and 62.0º) associated to non-basal planes (110) and (113).[17a]

Patterns recorded with calcined hydrotalcite (HTC) exhibit two broad reflections with low intensity at high 2θ angle (43.4º and 63.1º) associated with planes (400) and (440), which correspond to typical Mg-Al mixed oxides.[17a,24] Rehydrated hydrotalcite (HTR-I) exhibits patterns of diffraction similar to those obtained with HTS, although presenting low intensity of the basal planes (003), (006) and (009) (see Supporting Information, Figure S2).[20] On the other hand, hybrid samples exhibited different degrees of reconstruction, the largest being observed with sonication (HTR-M2), followed by samples obtained with magnetic stirring (HTR-M1). Finally, poorest reconstruction was achieved by mechanochemical activation (HTR-M3). Among sequential methods HTR-M4 to HTR-M6 materials, the lattest showed the major recovery of HT structure. Finally, sample HTR-M7 presented similar degree of reconstruction relative to that found in HTR-M6. Nevertheless, two additional small peaks (highlighted * in Figure 1) were observed, suggesting a different disposition of the amino acid on the interlaminar space (see Figure 1). [22d,22e,24b,25b]

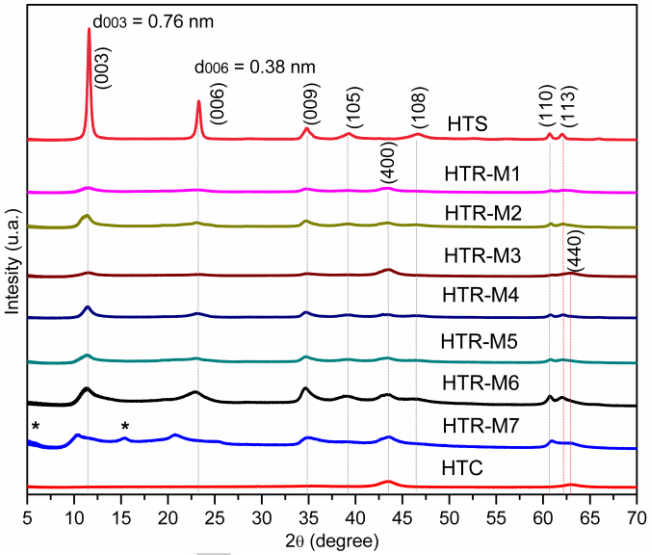

Figure 1. Powder X-ray diffractograms of pristine hydrotalcite (HTS), calcined material (HTC) and reconstructed hydrotalcite in presence of L-Phe, prepared according to the different approaches detailed in Table 1 (HTR-M1 to HTR-M7).

Based on these observations, method M6 was chosen as the best to optimize the incorporation of both α,β-dipeptides (H_2N-L-Val-*N*-Bn-β-Ala-COOH (**2**, α,β-L-Val) and H_2N-L-Leu-β-*N*-Bn-Ala-COOH (**3**, α,β-L-Leu)) and α-amino acids (D-phenylalanine (D-Phe, **4**) and L-tryptophan (L-Trp, **5**)) into the hydrotalcite structure.

The molecular structures of the chiral α-amino acids and α,β-dipeptides employed in this work are shown in Figure 2. Previously these free amino acids and α,β-dipeptides had proved to be highly efficient organocatalysts in asymmetric Michael addition reactions.[9b,d] According to powder XRD patterns for reconstructed hydrotalcite with amino acids (HTR-D-Phe, HTR-L-Phe and HTR-L-Trp) and α,β-dipeptides (HTR-α,β-L-Val and HTR-α,β-L-Leu) (see Figure 3), all samples incorporated the organic guest to essentially the same extent in the hydrotalcite structure and were associated to hydrotalcite type materials with low crystallinity, as indicated by broad and low intensity peaks of basal planes (003) and (006), which is in line with previous literature reports.[22d,22k]

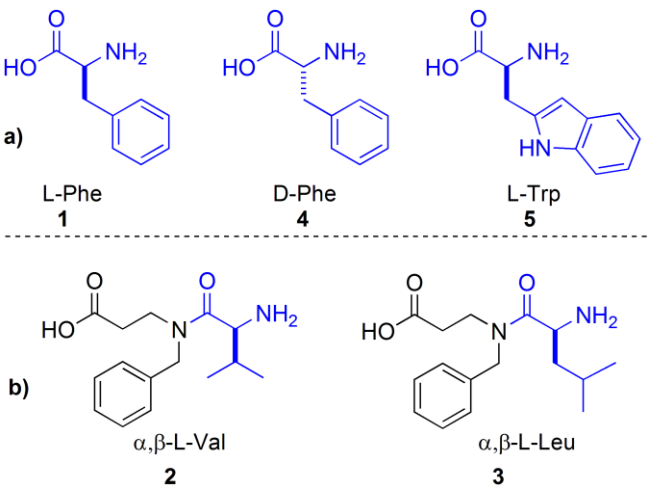

Figure 2. Molecular structures of a) *α-amino acid* (L-phenylalanine (**1,** L-Phe**)**, D-phenylalanine (**4**, D-Phe) and L-tryptophan (L-Trp, **5**)). b) α,β-dipeptides (H_2N-L-Val-*N*-Bn-β-Ala-COOH (**2,** α,β-L-Val) and H_2N-L-Leu-*N*-Bn-β-Ala-COOH (**3**, α,β-L-Leu)).

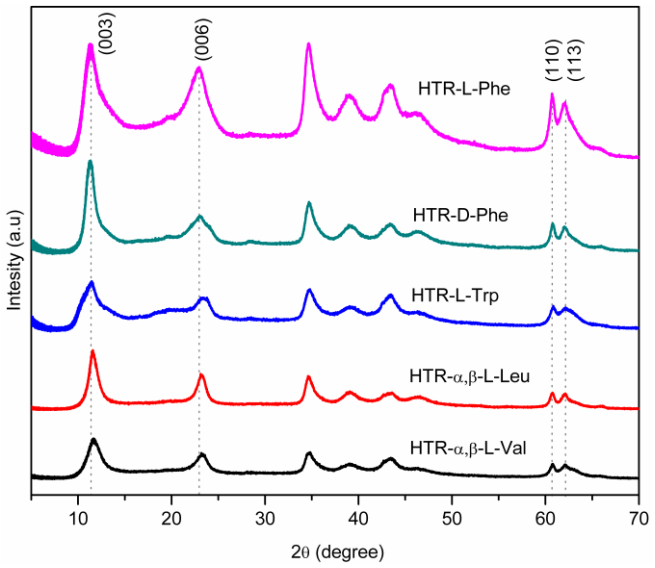

Figure 3. Powder X-ray diffractograms of reconstructed hydrotalcite (HTR) by method M6 in the presence of amino acid L-Phe (HTR-L-Phe), D-Phe (HTR-D-Phe), L-Trp (HTR-L-Trp), and α,β-dipeptides α,β-L-Leu (HTR-α,β-L-Leu) and α,β-L-Val (HTR-α,β-L-Val).

Basal spacing and interlayer space of the hydrotalcite-derived samples were measured according to Bragg's law using the peaks at basal planes (003) and (006), respectively. The results are summarized in Table 2. Basal spacing (d_{003}) corresponds to the distance between tops of two adjacent brucite type layers and interlayer space (d_{006}), also known as gallery height is the distance between top and bottom of two adjacent brucite-type layers. Taking reflection planes of HTS as reference, no apparent shift of (003) and (006) planes are noticed in all samples (*Cf*. Figures 1 and 3), which suggests similar distances of basal spacing and gallery height (Table 2, entries 1-7). On the other hand, basal layer corresponds to the thickness of brucite-type layer, and it was determined by the difference between basal spacing and interlayer space. The values calculated for all samples fall in the range of 0.38 to 0.39 nm. These relatively low values, less than 0.48 nm that is commonly found in basal layer of Mg/Al hydrotalcite are in line with data recently reported by Chao and coworkers.[22k]

It is clear then that the degree of intercalation of amino acids into the interlaminar space of HT is dependent on the method of preparation, reaction temperature, pH, and the concentration of the amino acids or peptide. These reaction parameters induce different arrangements (horizontal or vertical, mono- or bilayers) of the amino acid or peptide into the interlaminar space.[22,23,24]

Based on the recorded gallery heights, a horizontal disposition of the intercalated amino acid and α,β-dipeptides is proposed. Apparently, in such orientation the organic molecules can occupy a specific interlamellar site that avoids an energetically unfavorable increase of the gallery height. Alternatively, this orientation allocates the organic molecules near the laminar edges, as suggested by the studies of Palinko[25c] and Medina,[25b] respectively.

Table 2. Structural properties of hydrotalcite-type materials prepared in this work.

Entry	Catalyst	Basal spacing $d_{(003)}$ (nm) [a]	Interlayer space $d_{(006)}$ (nm) [b]	Amount Interlayer space (wt %)[c]
1	HTS	0.762	0.381	n.d.[d]
2	HTR-I	0.761	0.383	n.d.[d]
3	HTR-L-Phe	0.772	0.386	10.3
4	HTR-α,β-L-Val	0.762	0.382	12.1
5	HTR-α,β-L-Leu	0.764	0.384	14.7
6	HTR-L-Trp	0.770	0.384	17.5
7	HTR-D-Phe	0.780	0.386	8.7

[a] Calculated by Bragg's Law equation using the (003) plane. [b] Calculated by Bragg's Law equation using the (006) plane. [c] Determined by a calibration curve in PBS (pH = 2.1). [d] n.d. no determined.

The amount of organic species incorporated into hybrid catalysts is reported in Table 2 (For details see Supporting Information). In the case of HTR-L-Phe, the amount of incorporation turned out to be 10 weight percent of L-Phe (Table 2, entry 3). This means that for each 100 mg of HTR-L-Phe there are 10 mg of L-Phe, that is a relatively low value. This could be a consequence of associated to the high pH value that prevents major loading into material and restoration.

FTIR-ATR spectra of free L-Phenylalanine (L-Phe), calcined hydrotalcite (HTC), a 1:1 mixture HTC/L-Phe (homogenized by milling with mortar and pestle), L-Phe intercalated into hydrotalcite (HTR-Phe), and pristine hydrotalcite (HTS) are depicted in Figure 4. The FTIR spectrum of L-Phe presents typical vibration bands for N-H and C-H (2900-3300 cm^{-1}), NH_3^+ (1623 and 1494 cm^{-1}) and the carboxylate group (1556 and 1406 cm^{-1}) in amino acids. The spectrum of the mixture HTC/L-Phe presents major bands associated to L-Phe and minor bands associated to HTC, in the range of 1000 to 550 cm^{-1}.[17a,20] Furthermore, the FTIR spectrum of HTC shows characteristic bands assigned to mixed oxide Mg(AlO) at 3449 cm^{-1}, 1435 cm^{-1} and Metal-Oxygen (M-O) bonds. [17a,20] On the other hand, spectra of HTS and HTR-L-Phe exhibit bending vibrations at 1365 and 3027cm^{-1} ascribed to CO_3^{2-} and CO_3^{2-}–H_2O, respectively. The vibration at 1640 cm^{-1} was ascribed to interlayer water, while the bending bands at 929 cm^{-1} and 771 cm^{-1} were associated to Al-O, and the stretching bands 3415-3440 cm^{-1} were assigned to –OH and H_2O in interlaminar zone. Finally, the salient vibration at 1558 cm^{-1} was ascribed to the carboxylate group in L-Phe.[24b,-c] Comparison of the FTIR spectra of HTR-L-Phe and the homogeneous mixture HTC:L-Phe reveals major differences between them. The former is similar to typical HTS, whereas the latter is rather similar to free L-Phe. These results are in line with those obtained by powder DRX, corroborating the prevalence of the hydrotalcite structure after the incorporation of L-Phe.

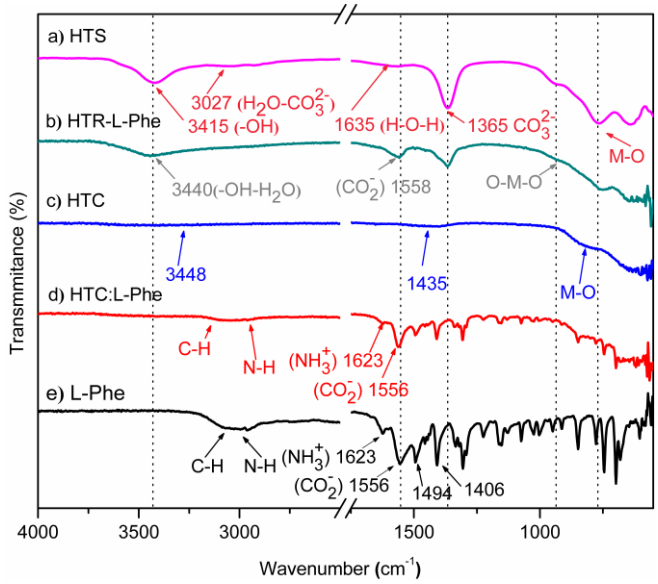

Figure 4. Comparison of FTIR-ATR spectra of a) pristine hydrotalcite (HTS), b) reconstructed hydrotalcite intercalated with L-phenylalanine (HTR-L-Phe), c) calcined hydrotalcite HTC, d) grinded mixture HTC:L-Phe (1:1), and e) free L-phenylalanine (L-Phe).

Catalytic evaluation of HT-derived materials in Michael addition reactions

Pristine and modified hydrotalcites were evaluated as catalysts in the Michael addition reaction between isobutyraldehyde **6a** and *N*-phenyl maleimide **7a**. It was decided to initiate the study employing our previously reported optimized reaction conditions;[9d] that is, under neat conditions using 5.5 mmol of the aldehyde **6a**, 0.5 mmol of the Michael acceptor **7a**, 30 mg of the hydrotalcite-derived materials, and a reaction time of 48 h at room temperature (Table 3, entries 1-6).

Pristine (HTS), calcined (HTC) and reconstructed hydrotalcite (HTR-I) were examined as heterogeneous bases lacking chirality. As it turned out, these materials afforded the anticipated Michael adducts as racemic mixtures in rather poor yields (2-8%) (Table 3, entries 1-3). By contrast, reconstructed hydrotalcites HTR-α,β-Val, HTR-α,β-Leu and HTR-L-Phe, that incorporate enantiopure α-amino acids or dipeptides containing functional groups able to activate one or both reaction components in the Michael addition reaction, exhibited much better performance, affording the expected addition products in 35-38% yield and good to excellent enantiomeric ratios in the range of 87:13 to 96:4 e.r. (Table 3, entries 5-6). According to these results, among all catalysts examined, HTR-L-Phe provided the best balance between yield and enantioselectivity. Therefore, this catalytic system was chosen to continue the optimization process. In particular, several catalyst and aldehyde loadings, and reaction times were evaluated. Salient results are summarized in Table 3 entries 7-16. Analysis of these results demonstrate that the best performance (87 % yield and 98:2 e.r.) was obtained with 1.75 mmol of isobutyraldehyde, 75 mg of HTR-L-Phe and 24 h of reaction time at ambient temperature (Table 3, entry 16).

Subsequently, catalytic materials HTR-D-Phe and HTR-L-Trp were evaluated under the optimized conditions (Table 3, entries 17 and 18). As anticipated, the catalyst HTR-D-Phe afforded similar yield and enantioselectivity but providing the product with opposite configuration (Table 3, entry 17). Interestingly, the catalytic material with a larger aryl moiety HTR-L-Trp did not provide better results than those obtained with HTR-L-Phe (Table 3, entries 16 and 18). Finally, it is worthy of mention that free L-phenylalanine (L-Phe) was not able to catalyze the Michael addition reaction under neat reaction conditions (Table 3, entry 19). This observation suggests that the conformational rigidity attained by confined amino acids and α,β-dipeptides in the hydrotalcite adducts plays an important role for the successful reaction under solvent free conditions. An additional advantage is that the present HT-derived catalysts, in contrast with previously reported work, avoid the use of harmful solvents such as CH_2Cl_2.[9b]

Table 3. Michael addition reaction of isobutyraldehyde to *N*-phenyl maleimide with various hydrotalcite-derived materials.

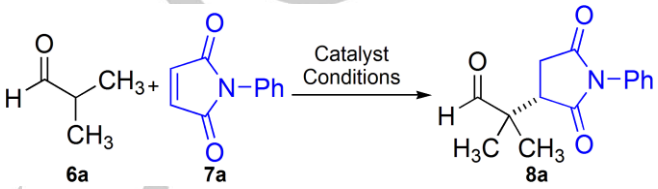

6a **7a** **8a**

Entry[a]	Catalyst	Amount (mg)	**6a** (mmol)	Time (h)[b]	Yield (%)[b]	e.r.[c]
1	HTS	30	5.5	48	2	50:50
2	HTC	30	5.5	48	3	50:50
3	HTR-I	30	5.5	48	2	50:50
4	HTR-L-Phe	30	5.5	48	35	96:4
5	HTR-α,β-L-Val	30	5.5	48	36	87:13
6	HTR-α,β-L-Leu	30	5.5	48	38	86:14
7	HTR-L-Phe	75	5.5	18	72	98:2
8	HTR-L-Phe	75	5.5	24	87	98:2
9	HTR-L-Phe	75	5.5	48	85	98:2
10	HTR-L-Phe	75	5.5	72	86	98:2
11	HTR-L-Phe	100	5.5	24	81	97:3
12	HTR-L-Phe	125	5. 5	24	86	96:4
13	HTR-L-Phe	150	5.5	24	88	90:10
14	HTR-L-Phe	75	1.0	24	79	98:2
15	HTR-L-Phe	75	1.5	24	82	98:2
16	HTR-L-Phe	75	1.75	24	87	98:2
17	HTR-D-Phe	75	1.75	24	82	2:98
18	HTR-L-Trp	75	1.75	24	83	96:4
19	L-Phe	8.2[d]	1.75	24	trace	n.d.

[a] Reaction conditions: isobutyraldehyde (**6a**, mmol), *N*-phenyl-maleimide (**7a**, 0.5 mmol), at room temperature. [b] Isolated yield. [c] Determined by chiral HPLC. [d] Equivalent to 10 mol%.

In spite of the fact that neat reaction conditions are considered environmental friendly, we decided to evaluate the effectiveness of the reaction in solution, since solvents can have a great influence in the reaction's yields, as well as in the stereoselectivity.[6d] The results from the screening of solvents are summarized shown in Table 4.

In contrast with observations reported by Kokotos,[9b] where the use of CH_2Cl_2 as solvent increased the reaction yield, here we observed lower yields relative to reactions under neat reaction conditions (Table 4, entry 1). On the other hand, the use of green solvents such as H_2O, MeOH and EtOAc gave good to excellent enantioselectivities, but rather poor yields relative to the reaction performed with CH_2Cl_2 (Table 4, entries 2-4). The use of low polarity solvents such as tetrahydrofuran, toluene and acetonitrile (Table 4, entries 5-7), and polar solvents such as DMSO, DMF and the mixture of DMF/H_2O (Table 4, entries 8-10) did not give any improvement. From these results, it is concluded that neat reaction conditions are superior to in-solution conditions (Table 4, entry 11 with entries 1-10).

Table 4. Solvent effect in the performance of the Michael addition reaction catalyzed by HTR-L-Phe.

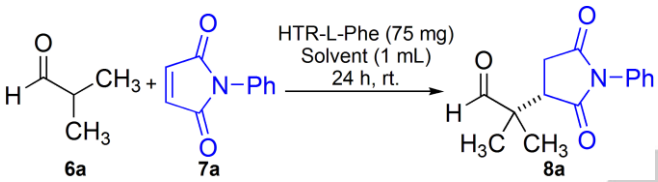

Entry[a]	Solvent	Yield (%)[b]	e.r.[c]
1	CH_2Cl_2	70	98:2
2	H_2O	23[d]	90:10
3	MeOH	40	98:2
4	EtOAc	39	98:2
5	THF	45	96:4
6	Toluene	55	98:2
7	CH_3CN	25	97:3
8	DMSO	60	89:11
9	DMF	35	94:6
10	DMF/H_2O	48	89:11
11	**neat**	**87**	**98:2**

[a] Reaction conditions: isobutyraldehyde (**6a**, 1.75 mmol), *N*-phenyl-maleimide (**7a**, 0.5 mmol), solvent (1 mL), 24 h at room temperature. [b] Isolated yield. [c] Enantiomeric ratio, determined by chiral HPLC.

Additionally, in order to improve the effectiveness of the reaction both in terms of yield and enantioselectivity, a screening of the potential influence of common additives including H-bond donors, or acids and bases (at 10 mol%) was carried out. Table 5 summarizes the most salient results. When urea, sulphamide and thiourea were evaluated as H-bond donors, the observed yields were 69%, 80% and 90%, respectively, whereas the recorded enantioselectivity was the same in the three cases, 97:3 (Table 5, entries 1-3). On the other hand, inorganic bases NaOH, KOH and Cs_2CO_3 did not improve the yield (82-84%), although the enantioselectivity was maintained (Table 5, entries 4-6). By contrast, organic bases such as DMAP afforded lower yield (16%) as well as lower enantioselectivity 91:9 (Table 5, entry 7). The lower yield could be the consequence of the formation of by-products. The presence of DABCO as additive affords better reaction yield (88%), but lower enantioselectivity, up to 95:5 e.r. (Table 5, entry 8). The use of imidazole as additive provided the Michael adduct in lower yield (74%) but good enantioselectivity, 97:3 (Table 5, entry 9). Finally, TFA and benzoic acid as additives did not improved the reaction yield but preserved the high enantioselectivity (Table 5, entries 10-11). It is worthy of mention that reaction times were shorter with sulphamide, DABCO and $PhCO_2H$. Nevertheless, the small increase in yield (1-4%) seems to be insufficient to justify the use of additives. Therefore, the best reaction conditions are those given in Table 4, entry 11.

Table 5. Screening of H-donors as additives in the asymmetric Michael addition reaction of isobutyraldehyde to *N*-phenylmaleimide catalyzed by HTR-L-Phe.

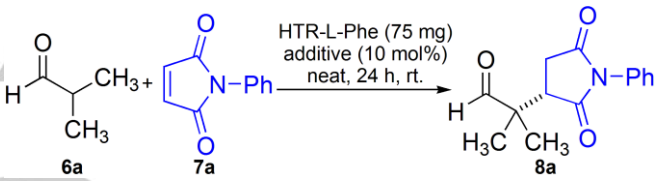

Entry[a]	Additive	Yield (%)[b]	e.r.[c]
1	Urea	69	97:3
2	Sulphamide	80	97:3
3	Thiourea	90	97:3
4	NaOH	82	98:2
5	KOH	82	97:3
6	Cs_2CO_3	84	97:7
7	DMAP	16	91:9
8	DABCO	88	95:5
9	Imidazole	74	97:3
10	TFA	78	97:3
11	$PhCO_2H$	85	97:3

[a] Experimental conditions: N-phenyl-maleimide (0.5 mmol), isobutyraldehyde (1.75 mmol), H-donor or additive (10 mol%), 24 h at room temperature. [b] Isolated yield. [c] Determined by chiral HPLC.

The scope of Michael addition reaction was evaluated with catalyst HTR-L-Phe under the optimized reaction conditions described in Table 4, entry 11, employing several *N*-substituted maleimides and aldehydes (Table 6). As it was previously mentioned, with catalyst HTR-D-Phe the enantiomer with opposite configuration is produced in 82% yield (compare entries 1 and 2 in Table 6). Halogenated derivatives of maleimides afford the expected products with high enantioselectivity (91:9 to 99:1 e.r.) and rather good yields (Table 6, entries 3-5). As anticipitated, the addition of

isobutyraldehyde **6a** to *N*-methyl maleimide **7e**, afforded the corresponding succinimide **8e** in high enantioselectivity (3:97) and slightly lower yield Table 6, entry 6. By contrast, introduction of ethyl groups in the aldehyde provided succinimide **8f** in 80% yield and excellent enantioselectivity (99:1 e.r.). Cyclohexanecarbaldehyde **6c** afforded product **8g** in 94% and 99:1 e.r. (Table 6, entry 8). Assignment of the absolute configuration of the Michael adducts **8a-g** was achieved by comparison with data reported in the literature.[6b,7a,9b]

Table 6. Scope of the Michael addition reaction of several aldehydes to *N*-substituted maleimides **7a-e**.

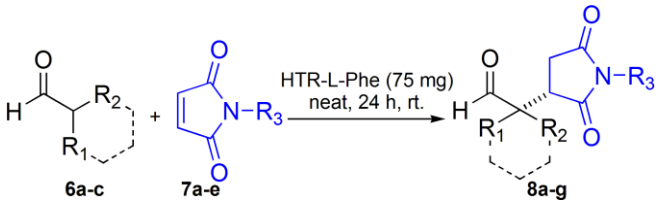

Entry[a]	Aldehyde R^1, R^2	Maleimide R^3	Michael adduct	Yield (%)[b]	e.r.[c]
1	Me, Me	Ph	**8a**	87	98:2
2	Me, Me	Ph	***ent*-8a**[d]	82	2:98
3	Me, Me	4-Br-Ph	**8b**	52	91:9
4	Me, Me	4-Cl-Ph	**8c**	86	99:1
5	Me, Me	3-Cl-Ph	**8d**	80	94:6
6	Me, Me	Me	**8e**	70	3:97
7	Et, Et	Ph	**8f**	80	99:1
8	$-(CH_2)_5-$	Ph	**8g**	94	99:1

[a] Reaction conditions: *N*-substituted-maleimide (0.5 mmol), aldehyde (1.75 mmol), 24 h at room temperature. [b] Isolated yield. [c] Determined by chiral HPLC. [d] HTR-D-Phe was used as catalyst

An important feature of the heterogenized organocatalysts reported herein is their easy separation (e.g. by filtration) and therefore the possibility of recycling. This represents an advantage from the economic and environmental points of view. With this in mind, recycling of the catalyst and large-scale reactions were evaluated. The results are summarized in Table 7.

In particular, catalyst HTR-L-Phe was removed from the reaction mixture by centrifugation-decantation, washed with ethyl acetate (2 x 2 mL) and ethanol (2 x 2.5 mL), and dried at 60 °C for 2 h under reduced pressure. The catalyst was carefully removed from the reaction medium, but a gradual loss of weight (5 - 8%) and catalytic activity was noticed after each recycle, affording **8a** in 45% of yield after the third cycle. Nevertheless, the high enantioselectivity of the reaction was maintained (Table 7, entries 1-4). The lower catalytic activity in the recovered catalyst can be attributed to a gradual deactivation of hydrotalcites material or leaching of the amino acid L-Phe, in the process of separation and recovery. Similar observations were reported in the deintercalation process of amino acids on hydrotalcites.[24a]

On the other hand, when larger scale, up to ten times larger, were carried out (5 mmol of **6a**), the results indicate that HTR-L-Phe can be reused with no significant loss of activity and enantioselectivity (Table 7, entry 5).

Table 7. Recycling of catalysts and large scale Michael addition reaction of isobutyraldehyde to *N*-phenyl maleimide.

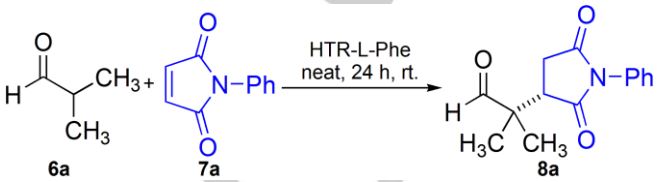

Entry[a]	Recycle of Catalyst	Yield (%)[b]	e.r.[c]
1	--	87	98:2
2	1	80	98:2
3	2	68	98:2
4	3	45	98:2
5	--	85[d]	98:2

[a] Unless otherwise specified the experimental conditions were *N*-phenyl-maleimide (0.5 mmol, 1 equiv.), isobutyraldehyde (3.5 equiv.), catalysts HTR-L-Phe (75 mg), neat, 24 h at room temperature. [b] Isolated yield. [c] Determined by chiral HPLC. [d] *N*-Phenyl-maleimide (5 mmol), isobutyraldehyde (17.5 mmol) and HTR-L-Phe (750 mg).

Based on previous reports where free α-amino acids and α,β-dipeptides have been used as organocatalysts,[9a,9d] a plausible enamine cycle is proposed for the catalytic process described herein (Scheme 1). Nucleophilic activation takes place following the condensation of isobutyraldehyde and L-phenylalanine giving rise to the well established enamine intermediate. Subsequently, the electrophilic maleimide is activated by coordination with the Lewis acidic hydrotalcite host and suitably positioned to react with the nucleophilic enamine. Following conjugate addition, the Michael product is liberated via hydrolysis of the iminium ion, and the cycle is begun again. It is worthy of mention that the hydrophobic character of the hydrotalcite interlayer space allows for the easy access of the reagents and establishes and adequate environment for a tight and ordered transition state, which induces the observed high enantioselectivities.

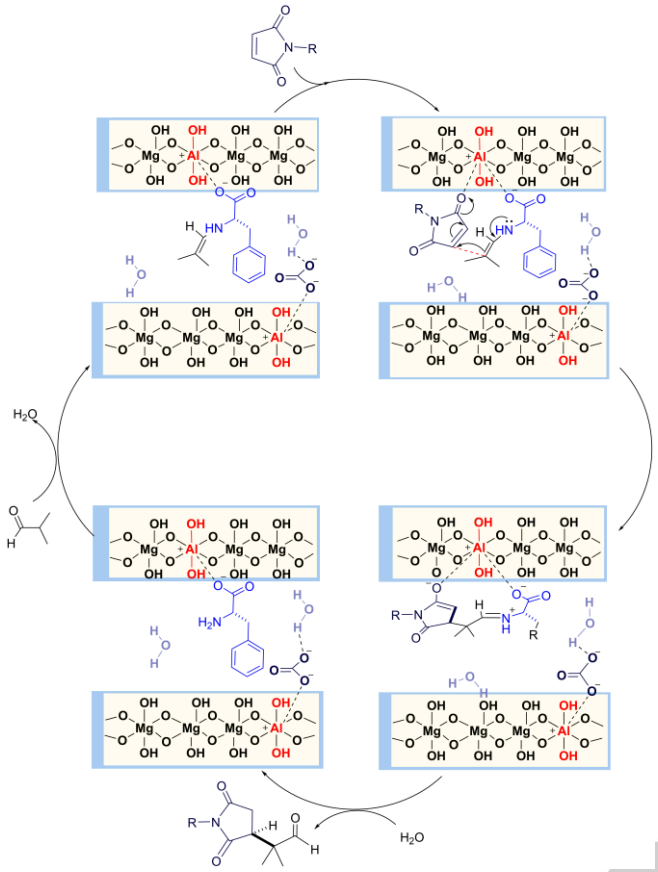

Scheme 1. Proposed catalytic cycle in the Michael addition reaction of L-Phe organocatalyst intercalated in hydrotalcite.

Conclusions

In summary, we have developed a simple an efficient protocol for the intercalation of α-amino acids and α,β-dipeptides into the interlamellar space of Mg/Al-hydrotalcites by the reconstruction method assisted by mechanochemical milling, ultrasound activation and mechanical stirring. Powder XRD analysis demonstrated the intercalation of the chiral molecules of interest, with a preferred horizontal arrangement between HT layers. The resulting hydrotalcite materials proved to be catalytically active in the asymmetric Michael addition reaction of isobutyraldehyde to *N*-phenyl-maleimide. Whereas pristine (HTS), calcined (HTC) and water-reconstructed (HTR-l) hydrotalcite alone afforded Michael adducts as racemic mixtures in very low yield (<3%), the organic-inorganic catalysts developed in this work exhibited good catalytic activity under solvent-free conditions, avoiding the usage of solvents and additives. Among the hybrid catalysts developed in this work, those incorporating α-amino acids afforded higher enantioselectivity (96:4 e.r. in average) relative to α,β-dipeptides (87:13 e.r. in average). In particular, HTR-L-Phe proved to be a most efficient organocatalyst affording highly enantioenriched substituted succinimides under solvent-free reaction conditions. Some of the advantages of this protocol are (1) easy preparation of the hybrid catalysts from commercial sources, (2) potential biodegradability of the hydrotalcite-derived catalytic materials, (3) easy recovery and reuse of the catalyst, and (4) the catalytic reaction does not require of additives nor solvents.

Experimental Section

Materials and apparatus

All reagents were purchased from Sigma-Aldrich and used as received unless otherwise indicated. Organic solvents (tetrahydrofuran, *N,N*-dimethyl formamide, methylene chloride, toluene, etc.) were reagent grade and purchased from Tecsiquim. Column chromatography was performed with Merck Silica Gel (0.040-0.063 mm). TLC were developed on Merck DC-F254 plates using UV light as revelator. Centrifuge Z-326-K (Hermle), operated to 3820 rpm at 5 °C. Sonication was performed on Bransonic ultrasonic cleaner 2510R-DTH. Calcination was carried out on a Muffle Furnace Thermolyne FB1415M. Mechanochemical activation was conducted on a Retsch MM200 ball mill, jar of PTFE (15 mL, 2.0 cm diameter) and two balls with core of stainless steel and cover of PTFE (1 cm diameter, mass 1.757 g), for 90 min at 25 Hz. UV-vis spectra were recorded in a PerkinElmer UV/vis spectrometer Lambda25, using Quartz cuvettes.

Characterization of hydrotalcite-derived materials. Powder X-ray patterns were recorded on Bruker D8 Advanced diffractometer, with Bragg-Brentano geometry, using Cu Kα (λ = 0.15418 nm) at 45 Kv and 20 mA, in the 2θ range of 3°–70°. FTIR spectra were recorded on a Varian 640-IR Spectrometer with diamond ATR accessory. Absorption spectra were recorded on Perkin Elmer UV/vis spectrometer Lambda25.

Characterization of organic compounds. NMR spectra were recorded on a JEOL ECA-500 spectrometer, and the chemical shifts were referenced to the deuterate solvent peak. Optical rotations were determined in an Anton Paar MCP-100 polarimeter using reagent grade solvents. Mass spectra (MS) were measured on a HPLC 1100 coupled to an MSD-TOF Agilent Technologies HR-MSTOF 1069A. Determination of enantiomeric excess was carried out on a Dionex HPLC Ultimate 3000 with UV/Visible detector, diode array, at 210 and 254 nm, using a suitable chiral column.

Synthesis of hydrotalcite type materials

Calcined hydrotalcite (HTC).[20] 10 g of commercial hydrotalcite Mg/Al (HTS, x = 0.333, Aldrich Id. No.652288) was placed in a porcelain capsule and calcined at 475 ºC (heat rate 20 ºC/min) for 8 h under static air atmosphere, then allowed to cool to room temperature to obtain 5.65 g of HTC as white powder. The sample was stored under N_2 atmosphere.

Reconstructed hydrotalcite in presence of water (HTR-l). An adequation of the standard procedure described elsewhere was followed.[20] In an Erlenmeyer flask of 50 mL equipped with stirring bar was added HTC (0.56 g) and decarbonated water (20 mL), and then the system was purged and fitted with N_2 atmosphere. The resulting solution was vigorously stirred at room temperature for 20 h. The resulting mixture was transferred to an Eppendorf flask of 50 mL and centrifuged at 3860 rpm for 20 min. The supernatant was decanted, and the remaining gel was dried under vacuum at 60 ºC for 3 h, followed by 12 h at room temperature to afford HTR-l (1.7 g) as a white powder.

Synthesis of α,β-dipeptides. H_2N-L-Val-*N*-Bn-β-Ala-COOH (**2**, α,β-L-Val) and H_2N-L-Leu-*N*-Bn-β-Ala -COOH (**3**, α,β-L-Leu) were prepared according to the procedure previously reported (See supporting information, Scheme S1).[26]

Reconstructed hydrotalcite in the presence of α-amino acids and α,β-dipeptides. (HTR-L-Phe). *Method M6*, into a jar of PTFE (15 mL, 2.0 cm diameter) equipped with two balls (each with core of stainless steel and cover of PTFE,1 cm diameter and mass 1.757 g) was added 0.56 g of HTC (~1.6 mmol), 0.46 g and L-Phe (2.8 mmol) and the resulting mixture was milled for 1 min at 25 Hz, before the addition of aqueous NaOH (1% w/w) to adjust pH 13. Milling was then continued for 90 min. The resulting suspension was transferred to an Erlenmeyer flask of 50 mL (equipped

with stirring bar and rubber septum), washing the jar with decarbonated water (15 mL), and purged with argon. The flask was immersed into an ultrasonic bath and sonicated for 60 min at 45 °C. The flask was then placed on a stirring plate and the reaction mixture was stirred for 20 h at room temperature. The resulting suspension was placed into an Eppendorf vial and centrifuged for 10 min, the supernatant was decanted, the remaining material was washed with decarbonated water (30 mL) and again centrifugated and decantated. This process was repeated until supernatant reached pH ~7. The remaining material was dried for 3 h at 60 °C under reduced pressure, followed of 12 h at room temperature. Affording 0.78 g of HTR-L-Phe as a white powder. A similar process was followed for the preparation of HTR-D-Phe, HTR-L-Trp, HTR-α,β-L-Val and HTR-α,β-L-Leu.

Determination of amino acid and α,β-dipeptide content in the hybrid catalysts. The concentration of amino acid and α,β-dipeptide into the hybrid catalysts was determined by means of calibration curves using UV-vis absorption spectra. Phosphate buffer solution (PBS, pH = 2.1) was used for all measurements. All calibration curves were plotted with average data from at least three sets of measurements made with solutions of amino acids (or α,β-dipeptides) in the range 20-300 μmol·L^{-1}. Hybrid catalysts (5 to 10 mg) were dissolved in 25 mL of PBS and stirred for 4 h at room temperature, before recording of UV-vis spectra. Absorption maxima for L-phenylalanine and D-phenylalanine were recorded at 207 nm, L-Tryptophan at 280 nm, and H_2N-L-Val-*N*-Bn-β-Ala-COOH and H_2N-L-Leu-*N*-Bnβ-Ala- COOH at 203 nm.

Catalyst evaluation in asymmetric Michael addition reactions

General catalyst evaluation in Michael addition reaction. Into a vial (8 mL) equipped with magnetic stirring bar and rubber septum, 86.5 mg (0.5 mmol, 1 equiv.) of *N*-phenyl maleimide and 75 mg of catalyst HTR-L-Phe was added. The vial was then capped before the dropwise addition of 0.16 mL (1.75 mmol, 3.5 equiv.) of isobutyraldehyde via syringe. The reaction mixture was stirred at room temperature for 24 h. Once the reaction was complete, (verified by TLC), in order to separate the catalyst from the crude reaction mixture, ethyl acetate (2 x 2.5 mL) was added and the resulting mixture was centrifuged for 5 min at 3820 rmp. The supernatant was decanted over a funnel with filter paper. The combined organic layers were concentrated under reduced pressure and the resulting crude product was purified by flash chromatographic column (hexanes/EtOAc, 7:3) affording 107 mg (87 % yield) of Michael adduct **8a** as a pale-yellow solid. Enantiomeric ratio (e.r.) was determined by chiral HPLC (see Supporting Information), and the absolute configuration of the Michael adducts (**8a-8g**) was assigned by comparison with literature data.[6b,7a,9a] The same procedure was conducted for the remaining aldehydes and *N*-substituted maleimides.

Acknowledgements

We are grateful to Consejo Nacional de Ciencia y Tecnología (CONACYT, Mexico) for financial support via grant No. A1-S-44097 and to fund SEP-CINVESTAV for financial support via grant 126. We also thank M. T. Cortez-Picasso for the recording of NMR spectra, M. A. Leiva-Ramirez for powder XRD analysis and G. Cuéllar-Rivera for MS-TOF analysis.

Conflict of Interest

The authors declare no conflict of interest.

Keywords: Asymmetric Michael addition • Ball milling • Green chemistry • Hydrotalcite• Supported catalysts

[1] a) S. B. Tsogoeva, *Eur. J. Org. Chem*. **2007**, *2007*, 1701–1716; b) T. Jerphagnon, M. G. Pizzuti, A. J. Minnaard, B. L. Feringa, *Chem. Soc. Rev*. **2009**, *38*, 1039–1075; c) Y. Zhang, W. Wang, *Catal. Sci. Technol.* **2012**, *2*, 42–53; d) M. Hayashi, R. Matsubara, *Tetrahedron Lett.* **2017**, *58*, 1793–1805; e). G. Koutoulogenis, N. Kaplaneris, C. G. Kokotos, *Beilstein J. Org. Chem.*, **2016**, *12*, 462-495.

[2] For reviews of asymmetric organocatalysis, see for example: a) J. Seayad, B. List, *Org. Biomol. Chem.* **2005**, *3*, 719–724; b) D. Enders, C. Grondal, M. R. M. Hüttl, *Angew. Chem., Int. Ed.* **2007**, *46*, 1570–1581; c) P. I. Dalko, "Comprehensive Enantioselective Organocatalysis: Catalysts, Reactions, and Applications", Wiley-VCH, Weinheim, **2013,** vol. 1–3; d) B. Han, X.-H. He, Y.-Q. Liu, G. He, C. Peng, J.-L. Li, *Chem. Soc. Rev.* **2021**, *50*, 1522–1586; e) E. Juaristi, *Tetrahedron* **2021**, 88, 132143. f) M. Tsakos, C. G. Kokotos, *Tetrahedron*, **2013**, *69*, 10199-10222.

[3] P. Chauhan, J. Kaur, S. S. Chimni, *Chem. Asian J.* **2013**, *8*, 328–346.

[4] a) K. Tang, J.-T. Zhang, *Neurol. Res.* **2002**, *24*, 473–478; b) C. Freiberg, H. P. Fischer, N. A. Brunner, *Antimicrob. Agents Chemother*. **2005**, *49*, 749–759; c) M. A. Silvers, G. T. Robertson, C. M. Taylor, G. L. Waldrop, *J. Med. Chem*. **2014**, *57*, 8947–8959; d) A. M. Hansen, G. Bonke, C. J. Larsen, N. Yavari, P. E. Nielsen, H. Franzyk, *Bioconjugate Chem.* **2016**, *27*, 863–867; e) S. E. Michalak, S. Nam, D. M. Kwon, D. A. Horne, C. D. Vanderwal, *J. Am. Chem. Soc.* **2019**, *141*, 9202–9206.

[5] G.-L. Zhao, Y. Xu, H. Sundén, L. Eriksson, M. Sayah, A. Córdova, *Chem. Commun.* **2007**, 734–735.

[6] a) F. Yu, Z. Jin, H. Huang, T. Ye, X. Liang, J. Ye, *Org. Biomol. Chem*. **2010**, *8*, 4767–4774; b) A. Avila, R. Chinchilla, E. Gómez-Bengoa, C. Nájera, *Tetrahedron: Asymmetry* **2013**, *24*, 1531–1535; c) J. Flores-Ferrándiz, R. Chinchilla, *Tetrahedron: Asymmetry* **2014**, *25*, 1091–1094.; d) J. Flores-Ferrándiz, B. Fiser, E. Gómez-Bengoa, R. Chinchilla, *Eur. J. Org. Chem*. **2015**, *2015*, 1218–1225; e) P. Vízcaíno-Milla, J. M. Sansano, C. Nájera, B. Fiser, E. Gómez-Bengoa, *Synthesis* **2015**, *47*, 2199–2206; f) T. de A. Fernandes, P. Vizcaíno-Milla, J. M. J. M. Ravasco, A. Ortega-Martínez, J. M. Sansano, C. Nájera, P. R. R. Costa, B. Fiser, E. Gómez-Bengoa, *Tetrahedron: Asymmetry* **2016**, *27*, 118–122; g) K. Nakashima, M. Kawada, S. Hirashima, A. Kosugi, M. Kato, A. Yoshida, Y. Koseki, T. Miura, *Tetrahedron: Asymmetry* **2016**, *27*, 888–895.

[7] a) A. Avila, R. Chinchilla, C. Nájera, *Tetrahedron: Asymmetry* **2012**, *23*, 1625–1627; b) A. Avila, R. Chinchilla, E. Gómez-Bengoa, C. Nájera, *Eur. J. Org. Chem*. **2013**, *23*, 5085–5092.

[8] a) F. Xue, L. Liu, S. Zhang, W. Duan, W. Wang, *Chem. Eur. J.* **2010**, *16*, 7979–7982; b) J.-F. Bai, L. Peng, L.-L. Wang, L.-X. Wang, X.-Y. Xu, *Tetrahedron* **2010**, *66*, 8928–8932; c) F. Yu, Z. Jin, H. Huang, T. Ye, X. Liang, J. Ye, *J. Org. Biomol. Chem.* **2010**, *8*, 4767–4774; d) T. Miura, A. Masuda, M. Ina, K. Nakashima, S. Nishida, N. Tada, A. Itoh, *Tetrahedron: Asymmetry* **2011**, *22*, 1605–1609; e) T. Miura, S. Nishida, A. Masuda, N. Tada, A. Itoh, *Tetrahedron Lett.* **2011**, *52*, 4158–4160; f) Z.-W. Ma, Y.-X. Liu, P.-L. Li, H. Ren, Y. Zhu, J.-C. Tao, *Tetrahedron: Asymmetry* **2011**, *22*, 1740–1748; g) J.-J. Wang, X.-J. Dong, W.-T. Wei, M. Yan, *Tetrahedron: Asymmetry* **2011**, *22*, 690–696; h) Z. T. Song, T. Zhang, H.-L. Du, Z.-W. Ma, C.-H. Zhang, J.-C. Tao, *Chirality* **2014**, *26*, 121–127.

[9] a) T. C. Nugent, A. Sadiq, A. Bibi, T. Heine, L. L. Zeonjuk, N. Vankova, B. S. Bassil, *Chem. Eur. J.* **2012**, *18*, 4088–4098; b) C. G. Kokotos, *Org. Lett.* **2013**, *15*, 2406–2409; c) C. E. Grünenfelder, J. K. Kisunzu, H. Wennemers, *Angew. Chem., Int. Ed.* **2016**, *55*, 8571–8574; d) C. G. Avila-Ortiz, L. Díaz-Corona, E. Jiménez-González, E. Juaristi, *Molecules* **2017**, 22, 1328; e) J. M. Landeros, L. Suchy, C. G. Ávila-Ortiz, N. Maulide, E. Juaristi, *Monatsh. Chem.* **2019**, *150*, 777–788; f) A. Schiza, N. Spiliopoulou, A. Shuha, C. G. Kokotos, *New J. Chem.*, **2018**, *42*, 18844-18849.

[10] a) S. Muramulla, J.-A. Ma, J. C.-G. Zhao, *Adv. Synth. Catal.* **2013**, *355*, 1260–1264; b) M. Durmaz, A. Sirit, *Tetrahedron: Asymmetry* **2013**, *24*, 1443–1448; c) W. Yang, K.-Z. Jiang, X. Lu, H.-M. Yang, L. Li, Y. Lu, L.-W. Xu, *Chem. Asian J.* **2013**, *8*, 1182–1190; d) Z.-W. Ma, X.-F Liu, J.-T. Liu, Z.-J. Liu, J.-C. Tao, *Tetrahedron Lett.* **2017**, *58*, 4487–4490; e) A. Torregrosa-Chinillach, A. Moragues, H. Pérez-Furundarena, R. Chinchilla, E. Gómez-Bengoa, G. Guillena, *Molecules* **2018**, *23*, 3299.

[11] a) R. A. Sheldon, *Green Chem*. **2007**, *9*, 1273–1283; b) P. Anastas, N. Eghbali, *Chem. Soc. Rev*. **2010**, *39*, 301–312.

[12] a) A. Bruckmann, A. Krebs, C. Bolm, *Green Chem*. **2008**, *10*, 1131–1141; b) J. G. Hernández, E. Juaristi, *Chem. Commun*. **2012**, *48*, 5396–5409; c) R. A. Sheldon, *Green Chem*. **2017**, *19*, 18–43; d) B. Karimi, M. Tavakolian, M. Akbari, F. Mansouri, *ChemCatChem* **2018**, *10*, 3173–3205.; e) M. Tavakolian, S. Vahdati-Khajeh, S. Asgari, *ChemCatChem* **2019**, *11*, 2943–2977; f) D. Krištofíková, V. Modrocká, M. Mečiarová, R. Šebesta. *ChemSusChem* **2020**, *13*, 2828–2858.

[13] a) J. Flores-Ferrándiz, R. Chinchilla. *Tetrahedron: Asymmetry* **2017**, *28*, 302–306; b) S. V. Kochetkov, A. S. Kucherenko S. G. Zlotin. *Mendeleev Commun*. **2017**, *27*, 473–475; c) A. Torregrosa-Chinillach, A. Sánchez-Laó, E. Santagostino, R. Chinchilla, *Molecules* **2019**, *24*, 4058.

[14] G. Szőllősi, V. Kozma, *ChemCatChem* **2018**, *10*, 4362–4368.

[15] V. Kozma, F. Fülöp, G. Szőllősi, *Adv. Synth. Catal.* **2020**, *362*, 2444–2458.

[16] a) C. Yu, J. He, *Chem. Commun*. **2012**, *48*, 4933–4940; b) S. B. Ötvös, I. Pálinkó, F. Fülöp, *Catal. Sci. Technol*. **2019**, *9*, 47–60.

[17] a) F. Cavani, F. Trifirò, A. Vaccari, *Catal. Today* **1991**, *11*, 173–301; b) F. L. Theiss, G. A. Ayoko, R. L. Frost, *Appl. Surf. Sci*. **2016**, *383*, 200–213; c) J. Qu, Q. Zhang, X. Li, X. He, S. Song, *Appl. Clay Sci*. **2016**, *119*, 185–192; d) M. V. Bukhtiyarova, *J. Solid State Chem*. **2019**, *269*, 494–506; e) G. Arrabito, A. Bonasera, G. Prestopino, A. Orsini, A. Mattoccia, E. Martinelli, B. Pignataro, P. G. Medaglia, *Crystals* **2019**, *9*, 361.

[18] a) V. Ambrogi, G. Fardella, G. Grandolini, L. Perioli, *Int. J. Pharm.* **2001**, *220*, 23–32; b) A. I. Khan, A. Ragavan, B. Fong, C. Markland, M. O'Brien, T. G. Dunbar, G. R. Williams, D. O'Hare, *Ind. Eng. Chem. Res*. **2009**, *48*, 10196–10205; c) M. L. Parello, R. Rojas, C. E. Giacomelli, *J. Colloid. Interface Sci*. **2010**, *351,* 134–139; d) R. Rojas, M. C. Palena, A. F. Jimenez-Kairuz, R. H. Manzo, C. E. Giacomelli, *Appl. Clay Sci*. **2012**, *62-63*, 15–20; e) V. Rives, M. del Arco, C. Martín, *Appl. Clay Sci.* **2014**, *88–89,* 239–269; f) S. Saha, S. Ray, R. Acharya, T. K. Chatterjee, J. Chakraborty, *Appl. Clay Sci*. **2017**, *135*, 493–509.; g) G. Mishra, B. Dash, S. Pandey, *Appl. Clay Sci*. **2018**, *153,* 172–186.

[19] a) B. M. Choudary, M. L. Kantam, V. Neeraja, K. Koteswara Rao, F. Figueras, L. Delmotte, *Green Chem*. **2001**, *3*, 257–260; b) P. Kumar Sahu, P. Kumar Sahu, R. Jain, R. Yadav, D. D. Agarwal, *Catal. Sci. Technol*. **2012**, *2*, 2465–2475.; c) M. Dixit, M. Mishra, P. A. Joshi, D. O. Shah, *Catal. Commun*. **2013**, *33*, 80–83; d) S. He, Z. An, M. Wei, D. G. Evans, X. Duan, *Chem. Commun*. **2013**, *49*, 5912–5920; e) G. Fan, F. Li, D. G. Evans, X. Duan, *Chem. Soc. Rev*. **2014**, *43*, 7040–7066; f) T. Baskaran, J. Christopher, A. Sakthivel, *RSC Adv*. **2015**, *5*, 98853–98875; g) O. Kikhtyanin, Z. Tišler, R. Velvarská, D. Kubička, *Appl. Catal. A* **2017**, *536*, 85–96.

[20] J. Sanchez-Valente, F. Figueras, M. Gravelle, P. Kumbhar, J. Lopez, J.-P. Besse, *J. Catal*. **2000**, *189*, 370–381.

[21] a) S. Aisawa, H. Hirahara, K. Ishiyama, W. Ogasawara, Y. Umetsu, E. Narita, *J. Solid State Chem*. **2003**, *174*, 342–348; b) M. L Kantam, R. Arundhathi, P. R. Likhar, D. Damodara, *Adv. Synth. Catal*. **2009**, *351*, 2633–2637; c) H. Nakayama, A. Hatakeyama, M. Tsuhako, *Int. J. Pharm.* **2010**, *393*, 105–112; d) H. Wang, X. Liu, Y. Wu, C. Hou, Y. Qiu, K. Guo, *Energy Fuels* **2017**, *31*, 9898−9904; e) J. Qu, X. He, Z. Lei, Q. Zhang, X. Liu, *Solid State Sci.* **2017**, *74*, 125–130; f) M. Miao, J. Wang, W. Hu, *Colloids Surf.* A **2018**, *543*, 144–154; g) S. G. Intasa-ard, K. J. Imwiset, S. Bureekaew, M. Ogawa, *Dalton Trans*. **2018**, *47*, 2896–2916.

[22] a) N. T. Whilton, P. J. Vickers, S. Mann. *J. Mater. Chem*, **1997**, *7*, 1623–1629; b) À. Fudala, I. Pálinkó, I. Kiricsi, *J. Mol. Struct*. **1999**, *482–483,* 33–37; c) S. Aisawa, S. Takahashi, W. Ogasawara, Y. Umetsu, E. Narita, *Clay Sci*. **2000**, *11*, 317–328; d) S. Aisawa, S. Takahashi, W. Ogasawara, Y. Umetsu, E. Narita, *J. Solid State Chem.* **2001**, *162*, 52–62; e) T. Hibino, *Chem. Mater*. **2004**, *16*, 5482–5488; f) Q. Yuan, M. Wei, Z. Wang, G. Wang, X. Duan, *Clays Clay Miner*. **2004**, *52*, 40–46; g) M. X. Reinholdt, R. J. Kirkpatrick, *Chem. Mater*. **2006**, *18*, 2567–2576; h) M. X. Reinholdt, P. K. Babu, R. J. Kirkpatrick, *J. Phys. Chem. C* **2009**, *113,* 3378–3381; i) M. Shamsayei, Y. Yamini, H. Asiabi, *J. Colloid. Interface. Sci.* **2018**, *529*, 255–264; j) B. M. Choudary, B. Kavita, N. S. Chowdari, B. Sreedhar, M. L. Kantam, *Catal. Lett.* **2002**, *78*, 373–377; k) H. N. Tran, C.-C. Lin, H.-P. Chao, *Sep. Purif. Technol.* **2018**, *192*, 36–45.

[23] a) À. Fudala, I. Pálinkó, B. Hrivnák, I. Kiricsi, *J. Therm. Anal. Calorim*. **1999**, *56*, 317–322; b) À. Fudala, I. Pálinkó, I. Kiricsi, *Inorg. Chem*. **1999**, *38*, 4653–4658; c) M. Wei, J. Guo, Z. Shi, Q. Yuan, M. Pu, G. Rao, X. Duan, *J. Mater. Sci.* **2007**, *42,* 2684–2689; d) M. Wei, M. Pu, J. Guo, J. Han, F. Li, J. He, D. G. Evans, X. Duan, *Chem. Mater*. **2008**, *20*, 5169–5180; e) X. Kong, L. Jin, M. Wei, X. Duan, *Appl. Clay Sci.* **2010***, 49,* 324–329; f) J. Wang, L. Zhao, H. Shi, J. He, *Angew. Chem. Int. Ed*. **2011**, *50*, 9171–9176; g) Y. Wang, P. Wu, B. Li, N. Zhu, Z. Dang, *Appl. Clay Sci*. **2011**, *53*, 615–620; h) L.-W. Zhao, H.-M. Shi, J.-Z. Wang, J. He, *Chem. Eur. J*. **2012**, *18*, 15323–15329; i) G. Choi, J.-H. Yang, G.-Y. Park, A. Vinu, A. Elzatahry, C. H. Yo, J.-H. Choy, *Eur. J. Inorg. Chem*. **2015**, 925–930; j) G. Varga, Á. Kukovecz, Z. Kónya, L. Korecz, S. Muráth, Z. Csendes, G. Peintler, S. Carlson, P. Sipos, I. Pálinkó, *J. Catal*. **2016**, *335*, 125–134.

[24] a) H. Nakayama, N. Wada, M. Tsuhako, *Int. J. Pharm*. **2004**, *269*, 469–478; b) S. Aisawa, H. Kudo, T. Hoshi, S. Takahashi, H. Hirahara, Y. Umetsu, E. Narita, *J. Solid State Chem*. **2004**, *177*, 3987–3994; c) Z. An, W. Zhang, H. Shi, J. He, *J. Catal*. **2006**, *241*, 319–327; e) S. Vijaikumar, A. Dhakshinamoorthy, K. Pitchumani, *Applied Catal. A* **2008**, *340,* 25–32; f) T. Subramanian, A. Dhakshinamoorthy, K. Pitchumani, *Tetrahedron Lett*. **2013**, *54,* 7167–7170; g) R.-A. Miranda, E. Finocchio, J. Llorca, F. Medina, G. Ramis, J. E. Sueiras, A. M. Segarra, *Phys. Chem. Chem. Phys*., **2013**, *15*, 15645–15659.

[25] a) R.-A. Miranda, J. Llorca, F. Medina, J. E. Sueiras, A. M. Segarra, *J. Catal.* **2011**, *282*, 65–73; b) D.-G. Crivoi, R.-A. Miranda, E. Finocchio, J. Llorca, G. Ramis, J. E. Sueiras, A. M. Segarra, F. Medina, *Appl. Catal. A* **2016**, *519*, 116–129; c) P. Sipos, I. Pálinkó *Catal. Today* **2018**, *306*, 32–41.

[26] E. Jiménez-González, C. G. Avila-Ortiz, R. González-Olvera, J. Vargas-Caporali, G. Dewynter, E. Juaristi, *Tetrahedron* **2012**, *68*, 9842–9852.

FULL PAPER

Entry for the Table of Contents

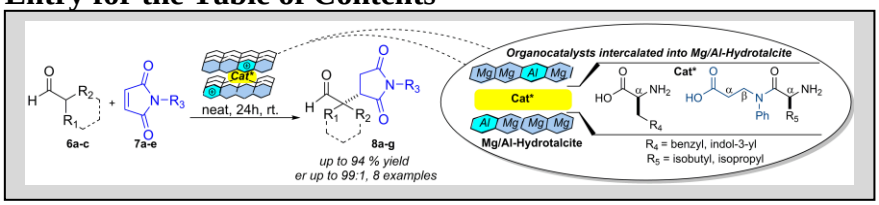

José M. Landeros,[a] Carlos Cruz-Hernández,[a] and Eusebio Juaristi*[a][b]*

Page No. – Page No.

α-Amino acids and α,β-dipeptides intercalated into hydrotalcite: efficient catalysts in the asymmetric Michael addition reaction of aldehydes to N-substituted maleimides

Recoverable hybrid materials for heterogeneous enantioselective organocatalyzed Michael addition reaction. Developed through the ready intercalation of α-amino acids and α,β-dipeptides into reconstructed hydrotalcite (Mg/Al) by means of sustainable technics such as mechanochemical and ultrasound activation. The conjugate addition of aldehydes to maleimides under mild and solvent free conditions proceeded with high yield and excellent enantioselectivity (up to 99:1 e.r.).